Electrodesorption Potentials of Self-Assembled Alkanethiolate Monolayers on Ag(111) and Au(111). An Electrochemical, Scanning Tunneling Microscopy and Density Functional Theory Study

O. Azzaroni,[†] M. E. Vela,[†] G. Andreasen,[†] P. Carro,[‡] and R. C. Salvarezza*[,‡,§]

Instituto de Investigaciones Fisicoquímicas Teóricas y Aplicadas (INIFTA), Universidad Nacional de La Plata - CONICET, Sucursal 4 Casilla de Correo 16 (1900) La Plata, Argentina, and Departamento de Química Física, Universidad de La Laguna, Tenerife, Spain

Received: August 27, 2002

Molecular interactions in well characterized self-assembled alkanethiolate monolayers on Au(111) and Ag(111) are studied from reductive electrodesorption curves recorded in 0.1 M NaOH in a 95% methanol +5% water mixture to minimize the effect of hydrophobic forces. From the electrochemical and STM data and quantum DFT calculations, it can be concluded that the difference in peak potentials experimentally observed for the reductive desorption of a given alkanethiolate from the Ag(111) and Au(111) surfaces is determined by the energy to introduce an electron into the adsorbed alkanethiolate−metal species, the desorption energy of the alkanethiolate anion, and the solvent/metal interaction energy.

Introduction

The understanding of molecular interactions that govern self-assembly processes is a key point in the development of nanoscience and nanotechnology. In this context, self-assembled monolayers (SAMs) of alkanethiolates on metals have attracted considerable scientific and technological interest because they provide a route to control corrosion, wetting, and wear properties of metal surfaces; to anchor different functional groups to be used as chemical and biochemical sensors;[1] to fabricate nanodevices for electronics;[2] to develop new nanofabrication methods;[3] and finally as model systems for interface science.[4]

Alkanethiolates adsorbed on Au(111) have been taken as a model system for SAM studies. It is well-known that the surface structure consists of an ordered $\sqrt{3} \times \sqrt{3}$ R30° lattice[1] and its related c(4 × 2) superlattice in both gas phase[5a] and liquid environments.[5b] In these lattices, the alkanethiolate molecules are chemisorbed on the Au surface by the S-heads forming a thiolate bond[1,6] and the tilt angle ranges from 20° to 40° with respect to the substrate normal.[7] The $\sqrt{3} \times \sqrt{3}$ R30° lattice exhibits nearest neighbor distances $d \approx 0.5$ nm[1], whereas the c(4 × 2) lattice exhibits some pairing of the S atoms as revealed by GIXD data.[4] Besides, STM measurements have shown $d =$ 0.45 nm between the bright and dark spots (interrows distance) and $d = 0.5$ nm inside the row (intrarow distance) of the c(4 × 2) superlattices.[5b]

In the case of alkanethiolate adsorption on Ag(111), chemisorbed molecules are also bonded by the S head to the Ag surface although their tilt angle with respect to the substrate normal ranges from 15° to 0°.[8a] Previous STM studies have shown that alkanethiolates with large hydrocarbon chains organize on Ag(111) forming an incommensurate hexagonal layer with $d = 0.46$ nm[8b] that is a value greater than $d = 0.44$ nm found in the distorted $\sqrt{7} \times \sqrt{7}$ R19.1° lattice observed for S on Ag(111) at a high surface coverage and for short alkanethiols on the same substrate.[9,10] Recent normal incidence X-ray standing wave (NIXSW) studies have shown that the S heads of octanethiol molecules in the $\sqrt{7} \times \sqrt{7}$ R19.1° lattice would be placed at hollow and top sites.[10] It should be noted that the value $d = 0.46$ nm has been observed in close packed bulk alkanes.

The self-assembly of these two-dimensional structures implies alkanethiolate−metal, alkanethiolate−alkanethiolate, alkanethiolate−environment, and metal−environment interactions. Previous studies for the alkanethiolate desorption from Au surfaces in hexadecane have reported activation energies that increase 0.84 kJ/mol per methylene unit.[11] Stabilization energies in the order of 1.5 kJ/mol per methylene unit have also been proposed from the analysis of different adsorption/desorption data.[12] In the case of electrolyte solutions, reductive electrodesorption curves have been used to estimate these contributions.[13] In aqueous 0.1 M NaOH, $\sqrt{3} \times \sqrt{3}$ R30° and c(4 × 2) alkanethiolate lattices on Au(111) are desorbed in sharp voltammetric peaks that shift in the negative potential (E) direction as the number of CH_2 units in the hydrocarbon chain (n) of alkanethiolate molecules increases. On the basis of peak potentials, the (E_p) vs n plots the stabilizing interactions, van der Waals and hydrophobic forces, have been estimated in 3−4 kJ/mol per methylene unit.[13,14] A detailed study on the reductive electrodesorption of SAMs on Ag(111) in aqueous and methanolic solutions has been also reported.[15] In aqueous solutions, the E_p vs n plots give similar results for hydrocarbon chain−chain and hydrocarbon chain−solvent interactions than those found for alkanethiolates on Au(111). It has been also shown that for a constant n the alkanethiolate molecules are desorbed from Ag(111) at more negative potential values than those corresponding for the desorption from Au(111). This difference has tentatively been explained by the smaller work function value of Ag than Au[13a] or to the stronger Lewis acid behavior of Ag than Au.[16]

* To whom correspondence should be addressed. E-mail: robsalva@inifta.unlp.edu.ar.
[†] Universidad Nacional de La Plata - CONICET.
[‡] Universidad de La Laguna.
[§] Visiting Professor from INIFTA, La Plata, Argentina.

10.1021/jp0219653 CCC: $22.00
Published on Web 00/00/0000 PAGE EST: 6.4

From the above discussion, it is evident that the surface structures of alkanethiolates on different metal surfaces are reasonably well established. Other basic aspects such as hydrocarbon chain length, solvent, and substrate effects on the adsorption/desorption of alkanethiolates have also been addressed in numerous studies. However, only a few of them have been concerned with the energetics of these processes. In those studies, large discrepancies from data reported by different laboratories have been observed and probably originated in subtle differences in the experimental conditions or surface preparation of the substrates.[12] Because of the potential technological applications of SAMs in aqueous media, quantitative aspects of the energetics involved in the adsorption/desorption of alkanethiolates on/at metal surfaces deserves further investigation. In this context, the understanding of the energetic contributions involved in the electrodesorption potentials becomes crucial because they determine the stability range of SAMs in aqueous media.

In this work, we have investigated the reductive electrodesorption of alkanethiolate lattices ($n \leq 16$) from Ag(111) and Au(111) surfaces using 0.1 M NaOH in 95% methanol +5% water as electrolyte under comparable experimental conditions. This electrolyte minimizes the contribution of hydrophobic forces in the adlayer stability,[15] and then it suppresses micelle formation that could complicate energetic calculations. We have found that the E_p vs n plots lead to a chain−chain interaction energy $E_{A-A} \approx 1.8 \pm 0.5$ kJ mol^{-1}/methylene unit and $E_{A-A} \approx 1.5 \pm 0.5$ kJ mol^{-1}/methylene unit for alkanethiolates on Ag(111) and Au(111), respectively. We propose that both the hexagonal lattice on Ag(111) and the c(4 × 2) lattice on Au(111) exhibit $d = 0.45-0.46$ nm in order to optimize hydrocarbon chain−hydrocarbon chain interactions. From the experimental data and quantum density functional theory calculations (DFT), it can be concluded that the difference in peak potentials experimentally observed for the reductive electrodesorption of a given alkanethiolate from different metals surfaces is determined by the energy to introduce an electron into the adsorbed alkanethiolate−metal species, the desorption energy of the alkanethiolate anion, and the solvent/metal interaction energy.

Experimental Section

Ag and Au arrandees were used as substrates for SAMs formation. The Ag and Au films were annealed in a hydrogen atmosphere at 300 and 400 °C, respectively. After annealing, the Ag and Au substrates were immersed for 20 hs in 5 mM X, (X = propanethiol, butanethiol, hexanethiol, dodecanethiol, and hexadecanethiol) methanolic solutions to form the SAM and rinsed for 1 h in methanol to eliminate multilayers. After adlayer formation, the surface structures were characterized by ex situ STM using a Nanoscope III STM (Digital Instruments Inc.). Images were taken in the constant current mode using Pt−Ir tips. Typical bias and tunneling currents were 0.1−1.0 V and 0.1−2 nA, respectively. The reductive electrodesorption of alkanethiolate adlayers was performed in a conventional three electrode glass cell containing 0.1 M NaOH in 95% methanol +5% water solution at a scan rate $\upsilon = 0.1$ V/s. A large area Pt counter electrode and saturated calomel as a reference electrode were used. Potentials in the text are referred to the saturated calomel electrode (SCE). All solutions were prepared with high purity chemicals.

Results

STM Characterization of Surface Structures. Typical ex situ STM images of the Ag substrate are shown in Figure 1.

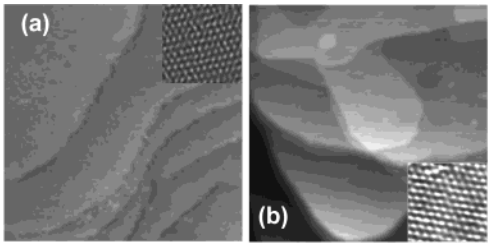

Figure 1. Typical (200 × 200 nm^2) STM images (raw data) of the (a) Ag(111) and (b) Au(111) films. These films exhibit smooth (111) terraces separated by monatomic high steps. The insets (3 × 3 nm^2) show atomic resolution of (a) Ag(111) and (b) Au(111) on the smooth terraces.

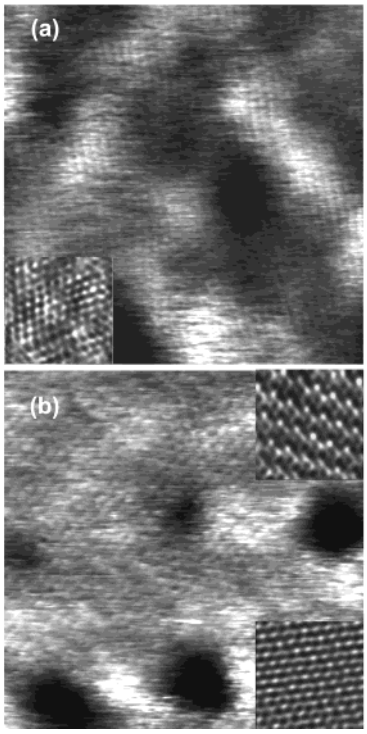

Figure 2. (a) (15 × 15 nm^2) STM image (raw data) of Ag(111) terraces covered by ordered domains of dodecanethiolate. The black regions correspond to monatomic deep holes. The inset (5 × 5 nm^2) shows the incommensurate hexagonal dodecanethiolate lattice on Ag(111). (b) (15 × 15 nm^2) STM image (raw data) of Au(111) terraces covered by ordered domains of dodecanethiolate. The black regions correspond to monatomic deep holes. The lower and upper insets (5 × 5 nm^2) show the $\sqrt{3} \times \sqrt{3}$ R30° and the c(4 × 2) dodecanethiol adlayers, respectively.

The vapor deposited Ag films on glass exhibit atomically smooth (111) terraces separated by monatomic high steps (Figure 1a). As already reported,[17] high-resolution STM images of fresh surfaces reveal the typical hexagonal pattern of the Ag(111) surface with nearest neighbor distance $d = 0.29$ nm (Figure 1a, inset). Similar images are obtained for the vapor deposited Au on glass (Figure 1b and inset).[18]

Ex situ STM images of dodecanethiol-covered Ag(111) and Au(111) prepared by immersion in the 5 mM dodecanethiol containing methanolic solutions are shown in Figure 2. At a low resolution, well ordered arrays of molecules and monatomic deep holes are observed for both alkanethiolate on Ag(111) (Figure 2a) and Au(111) (Figure 2b). At a high resolution, the STM images (Figure 2a inset) of the ordered dodecanethiolate domains on Ag(111) reveal the incommensurate hexagonal lattice with $d = 0.46$ nm.[8,19] On the other hand, for dodecanethiolate monolayers on Au(111), the surface structure consists

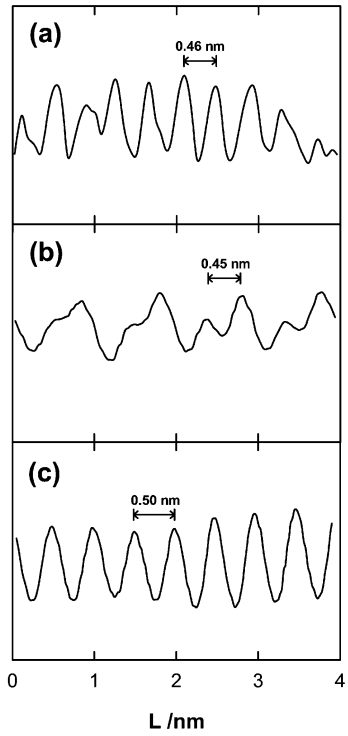

Figure 3. Cross-sections corresponding to (a) incommensurate hexagonal dodecanethiolate lattice on Ag(111), (b) c(4 × 2) dodecanethiolate adlayer on Au(111), and (c) $\sqrt{3} \times \sqrt{3}$ R30° dodecanethiolate adlayer on Au(111).

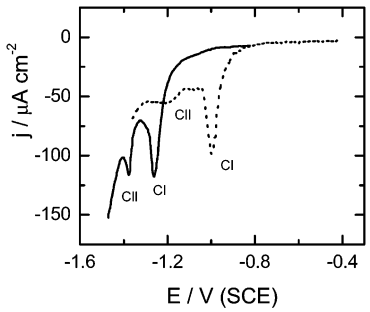

Figure 4. Current density (*j*) vs *E* profiles for the reductive electrodesorption of dodecanethiolate adlayers from the Ag(111) (solid line) and Au(111) (dotted line) surfaces recorded at $\upsilon = 0.1$ V s^{-1}. Electrolyte: 0.1 M NaOH in 95% methanol + 5% water solution.

of $\sqrt{3} \times \sqrt{3}$ R30° with $d = 0.5$ nm and its c(4 × 2) superlattice (Figure 2b insets) with $d = 0.45$ nm between dark and bright spots (interrows) and $d = 0.5$ nm inside the rows (intrarows; Figure 3).[5b]

Reductive Electrodesorption Curves. A typical current density (*j*) vs potential (*E*) profile for the reductive electrodesorption of the ordered hexagonal dodecanethiolate lattice from the Ag(111) surface in 0.1 M NaOH in 95% methanol + 5% water solution is shown in Figure 4 (solid line). The alkanethiolate lattice is mainly removed from the electrode surface at the current peak (CI) located −1.26 V (Figure 4) yielding alkanethiolate anions according to the global reaction

$$(CH_3)(CH_2)_nS{-}Me + \text{solvent} + e = [(CH_3)(CH_2)_nS^-]_{solv} + Me_{solv} \quad (1)$$

In eq 1, $(CH_3)(CH_2)_nS$ stands for the adsorbed alkanethiolate molecule on the Me substrate, $[(CH_3)(CH_2)_nS^-]_{solv}$ stands for the solvated desorbed alkanethiolate, and Me_{solv} stands for the solvated substrate. As already reported,[15] a small amount of dodecanethiolate, remaining on the Ag(111) surface, is removed at a small and broad current peak (CII) located at −1.38 V, just before the hydrogen evolution reaction. Similar profiles are recorded for the reductive electrodesorption of the propanethiolate, butanethiolate, hexanethiolate, and hexadecanethiolate lattices from the Ag(111) surface. The peak potential corresponding to current peak CI (E_p) shifts in the negative direction as the number of methylene units in the hydrocarbon chain (*n*) increases. The E_p vs *n* plot yields a straight line with a slope $b = 0.02 \pm 0.005$ V/CH_2 unit (Figure 5), the same value that has been reported in ref 15. Note that although the double layer charge could affect the voltammetric peak width[20] it has a negligible influence on the peak potential value.

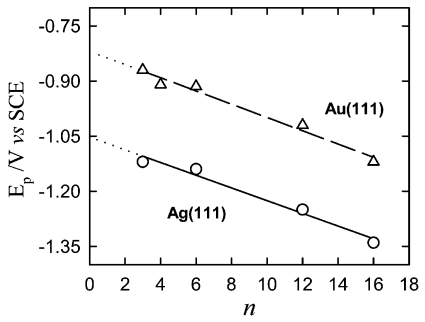

Figure 5. E_p vs *n* plots derived from the reductive electrodesorption curves ($\upsilon = 0.1$ V s^{-1}) recorded in 0.1 M NaOH in 95% methanol + 5% water solution. (○) Ag(111) and (△) Au(111). Dotted traces are the regression fitted lines extrapolated to $n = 0$. The error bars are smaller than the symbol size.

In the case of Ag, it has been reported that long immersion times result in the build up of a sulfur layer at the interface.[21] To address this point, we have made reductive electrodesorption of S-covered Ag electrodes prepared by immersion of the Ag substrate in 10^{-3} M Na_2S solution under comparable conditions. In this case, the reductive electrodesorption of the $\sqrt{7} \times \sqrt{7}$ R19.1° S lattice occurs at $E_p = -1.0$ V, well outside of the potential range where alkanethiolate ($3 \leq n \leq 16$) electrodesorption takes place. No traces of this peak were observed in the reductive electrodesorption curves of these alkanethiolates suggesting that no significant S contamination of SAMs are present in our samples. In the case of contaminated short alkanethiols ($n = 3{-}4$), we have clearly observed the S-electrodesorption peak.

We have also recorded *j* vs *E* profiles for the reductive electrodesorption of these alkanethiolates from the Au(111) surface in the same electrolyte. Although data for the reductive electrodesorption of dodecanethiolate monolayers in 0.5 M KOH in ethanol are available,[22] we have not found similar data for other alkanethiolates from Au(111) in low water-containing electrolytes. A typical reductive electrodesorption curve for dodecanethiolate from the Au(111) surface in this electrolyte is shown in Figure 4 (dotted line). The reductive desorption of the $\sqrt{3} \times \sqrt{3}$ R30° and c(4 × 2) lattices from the Au(111) surface takes place in the large single peak CI located at −1.0 V (Figure 4, dotted line) and a small peak (CII) at the negative potential side.[23] For peak CI, the analysis of E_p vs *n* plot for the reductive desorption of these ordered lattices from the Au(111) surface (Figure 5) also yields $b = 0.017 \pm 0.005$ V/CH_2 unit, which is a similar value than that obtained for the Ag(111) surface (within the experimental error) but lower than $b = 0.03$ V/CH_2 unit obtained for the reductive desorption of these lattices from the Au(111) surface in aqueous solutions.[14,15] The E_p vs *n* plot for alkanethiolate-covered Au(111) is shifted to more

positive potentials than that recorded for alkanethiolate-covered Ag(111); that is, the reductive electrodesorption of alkanethiolate lattices from the Ag(111) surface is more difficult than those from the Au(111) surface.

It should be noted that peak CII has been assigned either to a capacitive current produced by the charge of the double layer of the substrate after alkanethiolate electrodesorption[24] or to alkanethiolate electrodesorption from step edges or surface defects. In situ STM images after alkanethiolate reductive electrodesorption at peak CI shows that alkanethiolate molecules remain adsorbed at step edges.[25] Similar results have been reported for S desorption from step edges of Au(111).[26] It means that the electrodesorption of these species from step edges could contribute to the charge involved in peak CII.

Quantum Density Functional Theory (DFT) Calculations. The adsorption energies of negatively charged methanethiolate anions (CH_3S^-) on the Au(111) and Ag(111) surface sites were estimated by using DFT. We are interested in the adsorption energy of the negatively charged species because the reductive electrodesorption process in aqueous media results in alkanethiolate anion formation (eq 1). Note that while several papers have studied the adsorption of the neutral species on Au(111)[27−30] and a few on Ag (111),[29] no data are available about the adsorption energy of alkanethiolate anions on these surfaces.

The cluster model used to represent the metal surface was built with 10 atoms distributed 7 in the top layer and 3 in the second layer (Figure 6a). The metal−metal distance was maintained fixed to the bulk value of 0.2884 nm for gold and 0.2889 nm for silver.[31] The selected surface sites for the anion adsorption, namely, hollow hcp, hollow fcc, top, fcc-bridge, hcp-bridge, and bridge, are shown in Figure 6b. Note that hcp and fcc sites involve tetrahedrical and octahedrical geometries (Figure 6a), respectively, whereas the fcc-bridge and hcp-bridge are slightly off-centered sites from the bridge position (Figure 6b). The methanethiolate anion was oriented with the sulfur atom pointed toward the metal surface at a certain distance over the selected surface site. The S-Me distance (d) and the α angle defined between the C−S bond and the substrate normal were optimized. The rest of the anion geometry was held throughout the calculations in optimized values of the isolated anion.

DFT calculations are based in the three-parameter hybrid method proposed by Becke, associated with the gradient corrected correlation functional of Lee, Yang, and Parr, B3LYP.[32] The Ag and Au atoms have been described with 11 electrons, whereas the remainder of the atomic electron density was replaced by relativistic effective core potential (ECP) from Hay and Wadt, LANL1MB.[33] The nd^{10} $(n + 1)s^1$ valence shells, Ag $n = 4$ and Au $n = 5$, were treated explicitly with the basis set LANL1MB. S, C, and H atoms are described with the standard 6-31G(d) basis set,[34] which is split valence plus polarization quality. In all cases, the electronic state considered is taken as the lowest energy closed-shell configuration. The theoretical calculations were performed with the electronic structure software Gaussian 98.[35] We have also calculated the charge remaining in the S atom after methanethiolate adsorption by using Mulliken populations. These are used as a qualitative tool because of their well-known limitations.

The methanethiolate adsorption energy, E_{ads}, has been defined as

$$E_{ads} = E[Me_{10}SCH_3]^- - [E[Me_{10}] + E[SCH_3{}^-]] \quad (2)$$

where $E[Me_{10}SCH_3]^-$ is the total energy of $[Me_{10}SCH_3]^-$ with the parameters d and α optimized, $E[Me_{10}]$ is the energy for the metal cluster, and $E[SCH_3{}^-]$ is the energy of methanethiolate anion.

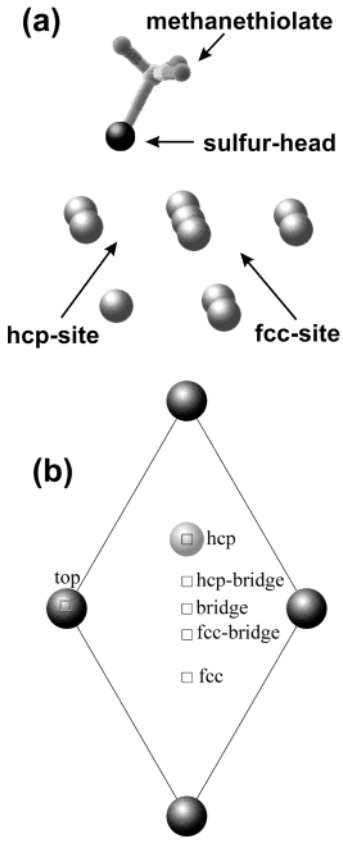

Figure 6. (a) Three-dimensional scheme (lateral view) showing the methanethiolate molecule on the Au(111) cluster used for DFT calculations. The hcp and fcc hollow sites are indicated. (b) Two-dimensional scheme (top view) showing the different adsorption Au(111) and Ag(111) sites (rectangles) used for the quantum DFT calculations. The Au atom in the second layer at the hcp site is indicated as a smaller gray circle. Note that the hcp-bridge and fcc-bridge are slightly off-centered from the bridge site.

TABLE 1: Desorption Energies ($-E_{ads}$), S−Me Bond Length (d), α Value, and the Charge of the S Atom for Methanethiolate Adsorption on the Different Au and Ag Sites

metal	site	d/ nm	α/ degrees	$-E_{ads}$/ kJ/mol	charge on the S atom
Au(111)	hcp	0.227	23.8	246	−0.13
	fcc	0.232	37.6	203	−0.15
	top	0.260	73.5	209	−0.21
	hcp-bridge	0.233	50.5	250	−0.16
	fcc-bridge	0.236	30	249	−0.18
	bridge	0.234	24.9	226	−0.18
Ag(111)	hcp	0.226	33.3	223	−0.28
	fcc	0.230	1.96	212	−0.28
	top	0.263	68.1	174	−0.31
	hcp-brigde	0.233	38.8	209	−0.28
	fcc-bridge	0.232	32.5	180	−0.30
	bridge	0.234	34.8	194	−0.29

Results obtained for the methanethiolate anion adsorption on Ag(111) and Au(111) surfaces are summarized in Table 1. S−Me bond lengths (d)[10] and α angles are similar to those calculated for methanethiol adsorption on Au(111) and Ag(111).[29,30] The magnitude of the E_{ads} value for methanethiolate adsorption on the different Ag(111) and Au(111) substrate sites agree with that experimentally reported[1] and with those estimated for negatively single charged anions adsorbed

on (111) faces.[36] The E_{ads} values differ no more than 40 kJ/mol for the different Ag(111) sites, with the hcp and hcp-bridge being the most stable. On the other hand, for the Au(111) surface hcp, hcp-brigde and fcc-bridge are the most stable sites with small energy differences among them. For the neutral species, the hcp site has been considered as the best site for alkanethiol adsorption on the Au(111) face.[27] However, recent DFT calculations have shown that the fcc site seems to be more stable than the hcp site.[37] On the other hand, other calculations have shown that short alkanethiol ($1 \le n \le 4$) adsorption is stronger at the fcc-bridge instead of at the fcc sites.[38] Differences smaller than 4 kJ/mol have been reported between methanethiolate adsorption at the fcc-brigde and bridge sites.[29] Similar adsorption energy values have been estimated for the adsorption of this species at the fcc-bridge and hcp-bridge sites.[30] The small adsorption energy differences reported for different sites, for both the negatively charged and neutral species, suggest that all of these sites are viable alternatives for adsorption. In the case of Au(111), the difference in E_{ads} for the different sites is 51 kJ/mol, i.e., greater than that observed for adsorption on the different Ag(111) sites. All Ag(111) sites exhibit E_{ads} values smaller than those calculated on the Au(111) surface, in contrast to that reported for the neutral $CH_3S^{\bullet}$.[29] Results also show that the S atom in the C−S−Ag bond has a greater negative charge than that of the S atom in the C−S−Au bond in agreement with XP spectroscopic data.[39]

For the most stable sites of the Au(111) and Ag(111) surfaces, we have also performed DFT calculations describing each metallic atom with 19 valence electrons $ns^2\ np^6\ nd^{10}\ (n+1)s^1$ valence shell, Ag $n = 4$ and Au $n = 5$, by using the effective core potential LanL2DZ and the standard LANL2DZ basis set, finding the same energy differences. To test cluster size effects, we have also done a single-point calculation of the energy in the most stable site on Au(111) and Ag(111) using 28 atoms distributed 18 in the top layer and 10 in the second layer. Again the adsorption energy differences between the most stable Au an Ag sites compare quite well with the data presented in Table 1.

Reaction [1] involves a charge transfer to a neutral alkanethiolate−Au species. The energetics of this step can be estimated from the energies ϵ_{LUMO} or ϵ_{HOMO}, the lowest unoccupied molecular orbital (LUMO), and the highest occupied molecular orbital (HOMO), respectively.[40] Thus, we performed a Hartree−Fock (HF) calculation for the most stable sites in the optimized geometry found previously in the DFT method. Thus, for the $[Au_{10}SCH_3]^-$ species at the hcp hollow site, we obtained $\epsilon_{HOMO} = -1.9482$ eV, whereas for $[Ag_{10}SCH_3]^-$ at the same site, we have −1.1605 eV; thus, $\Delta\epsilon_{HOMO} = 0.788$ eV = 76.00 kJ/mol. In the case of ϵ_{LUMO}, we have obtained for $[Au_{10}SCH_3]$ $\epsilon_{LUMO} = -1.431$ eV, and for $[Ag_{10}SCH_3]$, $\epsilon_{LUMO} = -0.706$ eV; thus, it results that $\Delta\epsilon_{LUMO} = 0.725$ eV = 70 kJ/mol.

Discussion

The reductive electrodesorption of alkanethiolate molecules from Au(111) and Ag(111) surfaces as alkanethiolate anions involves the nucleation and growth of holes in the adsorbed layer.[14,15] The energy barrier to desorb an alkanethiolate molecule from the edge of a growing hole should include the alkanethiolate−substrate (E_{A-S}), alkanethiolate−alkanethiolate (E_{A-A}), alkanethiolate−solvent (E_{A-s}), and substrate−solvent (E_{S-s}) interaction energies.[12,14]

The reductive desorption process of an adsorbed alkanethiolate molecule from a metal substrate (Me) in solvent *s* can be described by the following reaction steps

$$(CH_3)(CH_2)_nS{-}Me + e = [(CH_3)(CH_2)_nS{-}Me]^- \quad (3)$$

$$[(CH_3)(CH_2)_nS{-}Me]^- = (CH_3)(CH_2)_nS^- + Me \quad (4)$$

$$(CH_3)(CH_2)_nS^- + solvent = [(CH_3)(CH_2)_nS^-]_{solv} \quad (5)$$

$$Me + solvent = Me_{solv} \quad (6)$$

The energy involved in step [3] (E_{ct}) is related to the energy needed to introduce an electron into the alkanethiolate-metal system.[41] Step [4] involves E_{des}, $E_{des} = -E_{ads}$, the desorption energy of the alkanethiolate−Me species that is *n*-independent as already discussed.[1] Therefore, E_{A-S} contains both E_{ct} and E_{des}. Step [4] also involves the breaking of hydrocarbon chain-hydrocarbon chain interactions (E_{A-A}). Finally, steps [5] and [6] involve E_{A-s} and E_{S-s}, respectively. The energy (E_{ed}) involved in the electrodesorption process is

$$E_{ed} = E_{des} + E_{A-s} + E_{A-A} + E_{S-s} + E_{ct} \quad (7)$$

The energy difference (ΔE_{ed}) for the electrodesorption of a given alkanethiolate from Ag(111) and Au(111) is determined by

$$\Delta E^n_{ed} = E^n_{edAg} - E^n_{edAu} = \Delta E_{des} + \Delta E_{A-s} + \Delta E_{A-A} + \Delta E_{S-s} + \Delta E_{ct} \quad (8)$$

Note that the electrochemical potential relates to the free energy rather than the energy in the enthalpy sense. However, the entropic changes involved in going from ordered alkanethiolate lattices on the Ag(111)/Au(111) surfaces to solvated alkanethiolates in the methanolic solution should be similar. Thus, entropy contributions are canceled when we consider free energy differences in the reductive electrodesoption taking place on these metals.

For $n = 0$, the *n*-dependent terms ΔE_{A-s} and ΔE_{A-A} cancel so that eq 8 becomes

$$\Delta E^{n=0}_{ed} = \Delta E_{des} + \Delta E_{S-s} + \Delta E_{ct} \quad (9)$$

Taking $E_{des} = 250$ kJ/mol (Table 1) for the most stable sites (hcp/hcp-bridge/fcc bridge) for CH_3S^-−Au(111) ($\sqrt{3} \times \sqrt{3}$ R30°) and $E_{des} = 203$ kJ/mol averaging $[E_{des}(hcp) + E_{des}(top)]/3$ for the corresponding to CH_3S^-−Ag(111) ($\sqrt{7} \times \sqrt{7}$ R19.1°), it results in $\Delta E_{des} = -47$ kJ/mol. On the other hand, as a first approximation, one can consider $E_{ct} = -\phi$. Using $\phi_{Ag} = 428.78$ kJ/mol[42] and $\phi_{Au} = 509.5$ kJ/mol,[43] one obtains $\Delta E_{ct} = 80.7$ kJ/mol. We have used in eq 9 $\Delta E_{S-s} = -8$ kJ/mol from experimental data for methanol adsorption on the Ag(111) and Au(111) surfaces.[44] Note that we used a mixture of 95% methanol 5% water as electrolyte rather than pure methanol. However, for water, $\Delta E_{S-s} = -5$ kJ/mol have been estimated,[45] so that $\Delta E_{S-s} = -8$ kJ/mol for the mixture should be considered as a reasonable value. Introducing these figures into eq 9, one obtains $\Delta E^{n=0}_{ed} = 26$ kJ/mol = 0.27 eV. Therefore, considering the one electron-transfer process [eq 1], the estimated value for ΔE_p at $n = 0$ results in $\Delta E_p(n = 0) = 0.27$ V. This figure is larger than $\Delta E_p(n = 0) = 0.22$ V extrapolated from the E_p vs *n* plots ($4 \le n \le 16$) for alkanethiolate electrodesorption from the Ag(111) and Au(111) surfaces (Figure 5). Note that the use of $\Delta E_{ct} = -\Delta\phi = 80.7$ kJ/mol alone to determine ΔE_p leads to a very large discrepancy ($\Delta E_p(n = 0) = 0.83$ V) in relation to the experimentally estimated value. The energy involved in step [1] can be also estimated by taking $\Delta E_{ct} = \Delta\epsilon_{HOMO}$ or $\Delta E_{ct} =$

$\Delta\epsilon_{LUMO}$. From $\Delta\epsilon_{LUMO} = 70$ kJ/mol, it results $\Delta E_{ed}^{n=0} = 15$ kJ/mol and $\Delta E_p(n = 0) = 0.16$ V, a figure somewhat smaller than that experimentally observed. On the other hand, by using $\Delta\epsilon_{HOMO}$, it results in 76 kJ/mol, and one obtains $\Delta E_{ed}^{n=0} = 21$ kJ/mol and $\Delta E_p(n = 0) = 0.22$ V, in excellent agreement with the value derived from the experiments. It should be noted that $\Delta\epsilon_{HOMO}$ values have a clear physical meaning, and they can be considered as reliable ionization potentials as recently reported from DFT calculations.[40] It must be noted that the error involved in the $\Delta E_p(n = 0)$ measurements is at least two times smaller ($\approx$0.025 V) than the error introduced by the use of $\Delta\phi$ rather than $\Delta\epsilon_{HOMO}$. Therefore, we propose that in eq 9 ΔE_{ct} should be replaced by $\Delta\epsilon_{HOMO}$.. Thus, our results demonstrate that the ΔE_p value for alkanethiolate desorption from Ag(111) and Au(111) surfaces is mainly determined by ΔE_{des}, $\Delta\epsilon_{HOMO}$, and ΔE_{S-s} rather than by solely $\Delta\phi$, in contrast to early suggestions.[13a,16]

For the reductive electrodesorption of different alkanethiolates from the substrate Me in a given solvent the terms ΔE_{des}, $\Delta\epsilon_{HOMO}$, and ΔE_{S-s} cancel. Therefore, the energy difference ($\Delta E_{edMe}^{\delta n} = E_{Me}^{n_2} - E_{Me}^{n_1}$) for this process is given by the *n*-dependent terms

$$\Delta E_{edMe}^{\delta n} = \Delta E_{A-s} + \Delta E_{A-A} \qquad (10)$$

Note that we can neglect the *n*-dependent long-ranged adsorbate−substrate interactions at physisorbed micelles[20] because they are not formed in methanolic solutions.[46] Therefore, for a given substrate, the shift in the E_p value with *n* should reflect mainly ΔE_{A-s} and ΔE_{A-A} contributions. Defining χ^{Me} as the increment in electrodesorption energy per methylene unit and considering the corresponding slopes for E_P vs *n* plots, 0.02 V/CH_2 unit for alkanethiolate on Ag(111) and 0.017 V/CH_2 unit for alkanethiolate on Au(111), χ^{Me} results in 1.80 and 1.56 kJ/mol per methylene unit for Ag(111) and Au(111), respectively. For estimating these values, a one-electron transfer was assumed. Similar values have been reported for alkanethiolate desorption in nonaqueous media.[12,15] These values are smaller than $\chi^{Me} = 3-4$ kJ/mol per methylene unit obtained in aqueous solutions for SAMs on Ag(111) and Au(111) because of the alkanethiolate−methanol interaction energy that favors electrodesorption. In fact, it has been proposed that hydrophobic forces play a relevant role in SAMs stabilization in aqueous media.[15] Thus, for short alkanethiolates self-assembled in ethanolic solutions, the terms ΔE_{A-s} and ΔE_{S-s} should destabilize the SAMs resulting in incomplete surface structures as found for ethanethiol SAMs on Au(111).[47] The fact that the χ^{Me} value for both metals in the same environment is quite similar indicates that in average the energy contribution resulting from the molecular packing should be of the same magnitude.

Finally, it should be mentioned that real substrates include surface features such as terraces, steps, domain boundaries, and monatomic-depth holes (Figure 1) that could differ in reactivity for alkanethiolate electrodesorption.[48] These issues are not addressed in our DFT cluster calculations that could be related to desorption of a single molecule from a defect-free terrace. However, the estimated energies are related to E_p values corresponding to the main peak CI where in situ STM observations have shown alkanethiolate electrodesorption from terraces.[25] Therefore, one can conclude that our energetic approach could be only valid for alkanethiolate electrodesorption from terraces. The energetics of alkanethiolate electrodesorption from step edges or other surface defects should involve other contributions that are not included in our simplified model. Besides, SAM adsorption/desorption kinetics is complex and has shown multiple rate constants and regimes. These limitations suggest that more systematic theoretical and experimental work is needed for a complete understanding of the physical chemistry involved in these fascinating two-dimensional systems.

Conclusions

The reductive desorption behavior of self-assembled alkanethiolate monolayers on Au(111) and Ag(111) in a 0.1 M NaOH 95% methanol + 5% water mixture to minimize the effect of hydrophobic forces has been compared. From electrochemical and STM data and quantum DFT calculations for alkanethiolate adsorption, it can be concluded that the difference in peak potentials experimentally observed for the reductive desorption of a given alkanethiolate from the Ag(111) and Au(111) surfaces is mainly determined by the energy to introduce an electron into the adsorbed alkanethiolate−metal species, the desorption energy of the alkanethiolate anion, and the solvent/metal interaction energy.

Acknowledgment. This work was supported by the Agencia Nacional de Promoción Científica y Tecnológica (PICT 99-5030) and CONICET (PIP 0897; Argentina) and BQU2002-03249 (Spain). M.E.V. is a member of the research career of CIC. R.C.S. thanks DGICyES (SAB2000-157) for financial assistance. The authors thank Dr. Dirk Schroeer for kindly supplying the Ag arrandees.

References and Notes

(1) Ulman, A. *Chem. Rev.* **1996**, *96*, 1533 and references therein.

(2) Haag, R.; Rampi, A. M.; Holmlin, R. E.; Whitesides, G. M. *J. Am. Chem. Soc.* **1999**, *121*, 7895.

(3) Xia, Y.; Rogers, J. A.; Paul, K. E.; Whitesides, G. M. *Chem. Rev.* **1999**, *99*, 1823. Schilardi, P. L.; Azzaroni, O.; Salvarezza, R. C. *Langmuir* **2001**, *17*, 2747.

(4) Schreiber, F. *Prog. Surf. Sci*. **2000**, *65*, 151 and references therein.

(5) Anselmetti, D.; Baratoff, A.; Guntherodt, H. J.; Delamarche, E.; Michel, B.; Gerber, Ch.; Kang, H.; Wolf, H.; Ringsdorf, H. *Europhys. Lett.* **1994**, *27*, 365. (b) Terán, F. T.; Vela, M. E.; Salvarezza, R. C.; Arvia, A. J. *J. Chem. Phys*. **1998**, *109*, 5703.

(6) Zhong, C.-J.; Brush, R. C.; Anderegg, J.; Porter, M. D. *Langmuir* **1999**, *15*, 518. Vericat, C.; Vela, M. E.; Andreasen, G.; Salvarezza, R. C.; Vázquez, L.; Martín-Gago, J. A. *Langmuir* **2001**, *17*, 4919.

(7) Porter, M. D.; Bright, T. B.; Allara, D. L.; Chidsey, C. E. D. *J. Am. Chem. Soc.* **1987**, *109*, 3559. (b) Nuzzo, R. G.; Dubois, L. H.; Allara, D. L. *J. Am. Chem. Soc*. **1990**, *112*, 558. (c) Bryant, M. A.; Pemberton, J. E. *J. Am. Chem. Soc*. **1991**, *113*, 8284. (d) Hähner, G.; Wöll, C.; Buck, M.; Grunze, M. *Langmuir* **1993**, *9*, 1955.

(8) Nemetz, A.; Fischer, T.; Ulman, A.; Knoll, W. *J. Chem. Phys.* **1993**, *98*, 5912. (b) Dhirani, K. S.; Hines, A.; Fischer, A. J.; Ismail, O.; Guyot-Sionnest, P. *Langmuir* **1995**, *11*, 2609. (c) Fenter, P.; Eisenberg, P.; Li, J.; Camillone, N.; Bernasek, S.; Scoles, G.; Ramanarayanan, T. A.; Liang, *Langmuir* **1991**, *7*, 2013.

(9) Aloisi, G. D.; Cavallini, M.; Innocenti, M.; Foresti, M. L.; Pezzatini, G.; Guidelli, R. *J. Phys. Chem. B* **1997**, *101*, 4774.

(10) Rieley, H.; Kendall, G. K.; Jones, R. G.; Woodruff, D. P. *Langmuir* **1999**, *15*, 8856.

(11) Bain, C. D.; Troughton, E. B.; Tao, Y.; Evall, J.; Whitesides, G. M.; Nuzzo, R. G. *J. Am. Chem. Soc*. **1989**, *111*, 321.

(12) Schwartz, D. *Annu. Rev. Phys. Chem*. **2001**, *52*, 107.

(13) Widrig, C. A.; Chung, C.; Porter, M. D. *J. Electroanal. Chem.* **1991**, *310*, 335. (b) Walczak, M.; Alves, C. A.; Lamp, B. D.; Porter, M. D. *J. Electroanal. Chem.* **1995**, *396*, 103. (c) Zhong, C.-J.; Porter, M. D. *J. Electroanal. Chem.* **1997**, *425*, 147. (d) Walczak, M. M.; Chung, C.; Stole, S. M.; Widrig, C. A.; Porter, M. D. *J. Am. Chem. Soc.* **1991**, *113*, 2370.

(14) Vela, M. E.; Martin, H.; Vericat, C.; Andreasen, G.; Hernández-Creus, A.; Salvarezza, R. C. *J. Phys. Chem. B* **2000**, *104*, 11878.

(15) Hatchett, D. W.; White, H. S. *J. Phys. Chem.* **1996**, *100*, 9864. Hatchett, D. W.; Stevenson, K. J.; Lacy, W. B.; Harris, J. M.; White, H. S. *J. Am. Chem. Soc*. **1997**, *119*, 6596.

(16) Hatchett, D. W.; Uibel, R. H.; Stevenson, K. J.; Harris, J. M.; White, H. S. *J. Am. Chem. Soc*. **1998**, *120*, 1062.

(17) Mohtat, N.; Byloos, M.; Soucy, M.; Morin, S.; Morin, M. *J. Electroanal. Chem*. **2000**, *484*, 120.

(18) Vázquez, L.; Hernández Creus, A.; Carro, P.; Ocón, P.; Herrasti, P.; Palacio, C.; Vara, J. M.; Salvarezza, R. C.; Arvia, A. J. *J. Phys. Chem.* **1992**, *96*, 10454.

(19) Andreasen, G.; Vela, M. E.; Salvarezza, R. C.; Arvia, A. J. *Langmuir* **1997**, *13*, 6814.

(20) Heinz, R.; Rabe, J. P. *Langmuir* **1995**, *11*, 506.

(21) Kakiuchi, T.; Usui, H.; Hobara, D.; Yamamoto, M. *Langmuir* **2002**, *18*, 5231.

(22) Laibinis, P.; Whitesides, G. M.; Allara, D. L.; Tao, Y.-T.; Parikh, A. N.; Nuzzo, R. G. *J. Am. Chem. Soc.* **1991**, *113*, 7152.

(23) Weisshaar, D. E.; Lamp, B. D.; Porter, M. D. *J. Am. Chem. Soc.* **1992**, *114*, 5860.

(24) Wong, S.-W.; Porter, M. D. *J. Electroanal. Chem.* **2000**, *485*, 135.

(25) Yang, D. F.; Maznai, A.; Morin, M. *J. Phys. Chem. B* **1997**, *101*, 1158.

(26) Vericat, C.; Andreasen, G.; Vela, M. E.; Martin, H.; Salvarezza, R. C. *J. Chem. Phys.* **2001**, *115*, 6672.

(27) Vericat, C.; Andreasen, G.; Vela, M. E.; Salvarezza, R. C. *J. Phys. Chem. B* **2000**, *104*, 302. (b) Andreasen, G.; Vericat, C.; Vela, M. E.; Salvarezza, R. C. *J. Chem. Phys.* **1999**, *111*, 9457.

(28) Sellers, H.; Ulman, A.; Shnidman, Y.; Eilers, J. E. *J. Am. Chem. Soc.* **1993** *115*, 9389.

(29) Beardmore, K. M.; Kress, J. D.; Bishop, A. R.; Grombech-Jensen, N. *Synth. Met.* **1997**, *84*, 317. Beardmore, K. M.; Kress, J. D.; Gronbech-Jensen, N.; Bishop, A. R. *Chem. Phys. Lett.* **1998**, *286*, 40.

(30) Akinaga, Y.; Najajima, T.; Hirao, K. *J. Chem. Phys.* **2001**, *114*, 8555.

(31) Gottschalck, J.; Hammer, B. *J. Chem. Phys.* **2002**, *116*, 784.

(32) Kittel, C. *Introduction to Solid State Physics*, 6th ed.; Wiley: New York, 1966.

(33) Becke, A. D. *J. Chem. Phys.* **1993**, *98*, 5648.

(34) Hay, P.; Wadt, R. *J. Chem Phys*, **1985**, *82*, 299.

(35) Levine, I. N. *Quantum Chemistry*, 5th ed.; Prentice Hall, New Jersey, 2000; p 492.

(36) Frisch, M. J.; Trucks, G. W.; Schlegel, H. B.; Scuseria, G. E.; Robb, M. A.; Cheeseman, J. R.; Zakrzewski, V. G.; Montgomery, J. A., Jr.; Stratmann, R. E.; Burant, J. C.; Dapprich, S.; Millam, J. M.; Daniels, A. D.; Kudin, K. N.; Strain, M. C.; Farkas, O.; Tomasi, J.; Barone, V.; Cossi, M.; Cammi, R.; Mennucci, B.; Pomelli, C.; Adamo, C.; Clifford, S.; Ochterski, J.; Petersson, G. A.; Ayala, P. Y.; Cui, Q.; Morokuma, K.; Malick, D. K.; Rabuck, A. D.; Raghavachari, K.; Foresman, J. B.; Cioslowski, J.; Ortiz, J. V.; Stefanov, B. B.; Liu, G.; Liashenko, A.; Piskorz, P.; Komaromi, I.; Gomperts, R.; Martin, R. L.; Fox, D. J.; Keith, T.; Al-Laham, M. A.; Peng, C. Y.; Nanayakkara, A.; Gonzalez, C.; Challacombe, M.; Gill, P. M. W.; Johnson, B. G.; Chen, W.; Wong, M. W.; Andres, J. L.; Head-Gordon, M.; Replogle, E. S.; Pople, J. A. *Gaussian 98*; Gaussian, Inc.: Pittsburgh, PA, 1998.

(37) Paredes Olivera, P.; Patrito, E. M.; Sellers, H. *Surf. Sci.* **1998**, *418*, 376.

(38) Yourdshahyan, Y.; Rappe, A. M. *J. Chem. Phys.* **2002**, *117*, 825. (b) Yourdshahyan, Y.; Zhang, H. K.; Rappe, A. M. *Phys. Rev. B* **2001**, *63*, 081405−1.

(39) Morikawa, Y.; Hayashi, T.; Liew, C. C.; Nozoye, H. *Surf. Sci.* **2002**, *507−510*, 46.

(40) Bensebaa, F.; Zhou, Y.; Deslandes, Y.; Kruus, E.; Ellis, T. H. *Surf. Sci.* **1998**, *405*, L472.

(41) Chong, D. P.; Gritsenko, O. V.; Baerends, E. J. *J. Chem. Phys.* **2002**, *116*, 1760.

(42) Sellers, H.; Patrito, E. M.; Paredes Olivera, P. *Surf. Sci.* **1996**, *356*, 222.

(43) Halley, J. W.; Walbran, S. In *Interfacial Electrochemistry*; Wieckowski, A., Ed.; Marcel Dekker Inc.: New York, 1999; p 9.

(44) Pirug, G.; Bonzel, H. P. In *Interfacial Electrochemistry*; Wieckowski, A., Ed.; Marcel Dekker Inc.: New York, 1999; p 270.

(45) Sexton, B. A.; Hughes, A. E. *Surf. Sci.* **1984**, *140*, 227.

(46) Kuznetsov, A.; Maslii, A. N.; Shapnik, M. S. *Russ. J. Electrochem.* **2000**, *36*, 1309.

(47) Hobara, D.; Miyake, K.; Imabayashi, S.; Niki, K.; Kakiuchi, T. *Langmuir* **1998**, *14*, 3590.

(48) Hagenström, H.; Schneeweiss, M. A.; Kolb, D. M. *Langmuir* **1999**, *15*, 2435.

(49) Martin, H.; Vericat, C.; Andreasen, G.; Vela, M. E.; Salvarezza, R. C. *J. Chem. Phys.* **2002**, *117*, 2293.